Physical model of an oboe: comparison with experiments

André Almeida[1], Christophe Vergez[2], René Caussé[1], Xavier Rodet[1]

[1]IRCAM - CNRS; 1, Place Igor Stravinsky; 75004 Paris FRANCE
[2]LMA - CNRS ; 31, chemin Joseph Aiguier; 13402 Marseille

almeida@ircam.fr, vergez@lma.cnrs-mrs.fr, causse@ircam.fr, rod@ircam.fr

Abstract

We propose a model which tries to take into account the differences between double-reed instruments and typical single reed models. These differences are identified from experiments on real double-reed instruments. Experimental data also allow the estimation of physical parameters to be introduced into a real-time sound synthesis model.

1. Introduction

Recent work on double reed instruments ([1] and [2]) sheds new light on the physical behavior of the reed. Observational data allow the validation of theoretical hypothesis on double reeds ([3] and [4]).

In this paper we propose a flexible real-time model of a double-reed instrument that can be adapted to the knowledge acquired by on-going experimental research on a real instrument. These experiments can provide both values of physical parameters of the model and newer refinements to the mathematical model from which the simulations are derived

2. Mathematical Model

The conception of a wind instrument model is usually based on the assumption that the reed and the bore of the instrument can be described independently. Their only interaction is made through two variables which can be considered homogeneous on a surface between the reed and the bore. In a one-dimensional model, these are the acoustically significant variables, pressure p and volume flow q.

2.1. Reed

Both blades of a double reed are considered to be equivalent (based on experimental observations already published [5]) and to have symmetric displacement. Therefore, only one blade needs to be modeled as a harmonic oscillator with a mass m, stiffness k and damping r. Its position at rest is noted H. The distance between the two blades of the double reed is thus obtained by doubling the position of the single harmonic oscillator. The pressure and position of the lips of the player against the reed

blades act as control parameters which only influence the reed position at rest H^1. The only external force applied to the reed are then due to the pressure difference between the mouth p_m and the inside of the reed p_r.

$$m\frac{\partial^2 z(t)}{\partial t^2} + r\frac{\partial z(t)}{\partial t} + k|z(t) - H|^\beta = p_r(t) - p_m \quad (1)$$

where the usual mass and damping have been implicitly divided by the reed effective area, yielding m and r. The stiffness law (usually $\Delta p = k \times (z(t) - H)$) is replaced here by a power law ($\Delta p = k(z(t) - H)^\beta$), since the experimental data does not fit to a linear law, as we shall see in section 3.

The right-hand side of equation 1 is the pressure difference between the inside of the reed and the mouth (the latter considered constant).

2.2. Flow

The same pressure difference affecting the reed ($p_m - p_r$) also creates a flow entering the reed. A simplified description of this flow is obtained using the Bernoulli theorem. The volume flow is calculated from the velocity by considering that the velocity is homogeneous over the reed entrance section ($S_{in}(z)$ – depending on the reed position z).

$$q(t) = \sqrt{2\frac{|p_m - p_r(t)|}{\rho}}S_{in}(z(t))$$
$$[1 + \text{sign}(z(t))]\,\text{sign}(p_m - p_r(t)) \quad (2)$$

The opening area of the reed $S_{in}(z(t))$ is proportional to the reed coordinate $z(t)$. In fact it is calculated as:

$$S_{in}(z(t)) = \alpha\gamma l_r z(t) \quad (3)$$

γ is the geometrical coefficient obtained in [1] by image analysis of a real double reed. It expresses the fact that the reed entrance is not a rectangle. α is the *Vena Contracta* coefficient.

---

[1]Lips may also affect the other parameters of the reed, such as the effective mass or damping.

Equation 2 corresponds to the simplest model that reproduces the behavior of a reed exciter if we consider that the reed pressure $p_r(t)$ is the acoustic input to the bore. Such an assumption is justified for reed instruments such as the clarinet, where the jet formed at the reed entrance completely dissipates its energy in the embouchure chamber of the clarinet. However, the geometry of a double reed suggests that more complex phenomena might arise in the flow within the reed. As proposed in [4], these phenomena can be modelized by the following formula, using an averaging approximation:

$$p_r(t) = p(t) + \frac{\rho}{2}\Psi\left(\frac{q(t)}{S_{ra}}\right)^2 \tag{4}$$

It relates the pressure at the beginning of the reed ($p_r(t)$) to the acoustic input pressure to the bore ($p(t)$). Ψ is a phenomenological coefficient which expresses the importance of the flow differences from a clarinet embouchure. S_{ra} is a cross-section area averaged throughout the reed.

2.3. Resonator

The resonator, assumed to have a linear response, is usually described either by its input impedance $Z_{in}(\omega)$ or by its reflection function $r(t)$.

Rather than using the reflection function, which relates the present value of the incoming pressure wave to the past values of the outgoing one, we propose to use an expression relating present and past values of pressure and flow. This allows easier interaction between experiments, modeling and simulation. The generic form of a resonator is:

$$\mathcal{Q}\left(q(t)\right) = \mathcal{P}\left(p(t)\right) \tag{5}$$

$\mathcal{P}$ and $\mathcal{Q}$ are differential operators applied to pressure p and flow q. They can be determined using the acoustic impedance $Z_i(\omega)$. As shown in section 4.1.3, the total number of coefficients used in the discrete version of equation 5 is kept rather small.

As an example, for an ideal cylindrical resonator, equation 5 becomes:

$$p(t) + p(t-\tau) = Z_0\left(q(t) - q(t-\tau)\right) \tag{6}$$

and for a conical one

$$\frac{S(r_1)}{\rho c}\left(\left(\frac{\partial p}{\partial t}\right)_t + \left(\frac{\partial p}{\partial t}\right)_{t-\tau}\right) +$$
$$\frac{S(r_1)}{\rho r_1}\left((p)_t - (p)_{t-\tau}\right) = \left(\frac{\partial q}{\partial t}\right)_t - \left(\frac{\partial q}{\partial t}\right)_{t-\tau} \tag{7}$$

with $\tau = 2l_t/c$ the back and forth path time inside the resonator, where l_t is the resonator length. In this expression, r_1 is the distance of the truncation point to the apex of the cone and $S(r)$ is the cone cross-section at distance r form the apex.

3. Parameters

The model described in section 2 requires the knowledge of a number of physical parameters which are not easy to measure. They are estimated experimentally.

3.1. Reed parameters

The stiffness law of the reed (see sect. 2.1) must be determined using a setup which resembles as much as possible that of a playing regime. This means for instance that the force must be evenly distributed over the reed surface rather than being applied at a single point. The simplest way to achieve this is to use air pressure applied only to the exterior face of both blades.

The experiment which we devised uses a similar setup as the one we use to estimate the reed characteristic ([2]), but we cover the reed entrance with a flexible transparent film to stop the flow. This way the only force acting upon the reed is the mouth pressure. The reed displacement is measured from the images of the slit entrance synchronized with the measured pressure.
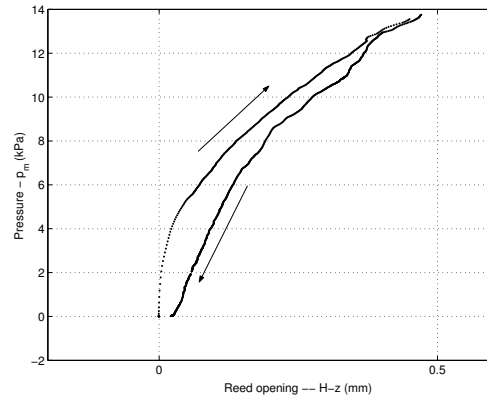

Figure 1: Reed position versus pressure difference applied between the reed's inside and outside while preventing any flow

Figure 1 shows the data resulting of an experiment where we slowly increased the pressure until the reed closed completely and then decreased it again to 0. The reed follows a different path while pressure is being increased or decreased. At the end of the experiment the reed is more closed than it was at the beginning. This suggests that there might be some visco-elastic effect influencing the reed position, although the pressure was increased and decreased very slowly. This fact was also observed on clarinet reeds [6].

As a preliminary test, we chose to build a stiffness model based on the increasing pressure curve, because it was aligned with the reed's position at rest. From this curve we estimated the following power law (written in S.I. units), as shown in figure 2:
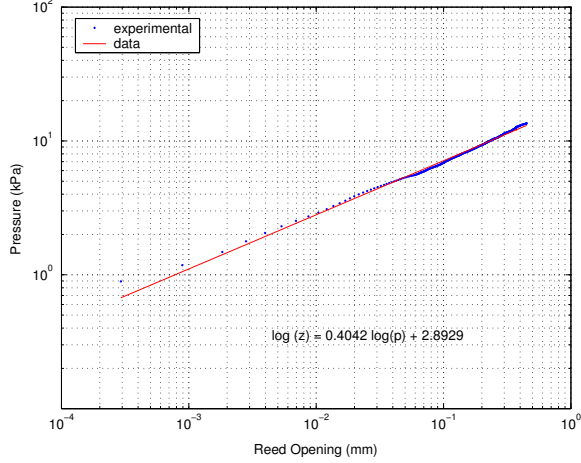
Figure 2: Reed displacement as a function of pressure applied to the reed

Figure 3: Fitting of the model of section 2 to the available p/q characteristic data

$$\Delta p = 2.85 \cdot 10^5 |z - H|^{0.4} \qquad (8)$$

This power law replaces the linear spring model usually used in classical reed models, in order to test its relevance in sound synthesis. Mass and damping coefficients can also be estimated from dynamic measurements. At present, we estimate them from theoretical considerations.

3.2. Estimation of Ψ coefficient

Ψ is an important phenomenological parameter in our simulations (see sect. 2.2), since it might introduce qualitative changes in the shape of the reed characteristic, such as hysteresis, as shown in [4]. By comparing this theoretical characteristic curve to one measured on a real instrument we can infer a value for this coefficient.

The measurement of the characteristic curve is described in [2]. We measure simultaneously the pressure difference between the mouth and the inside of the reed and the flow, by means of a calibrated diaphragm covering the output of the double reed. We represent the measured points (circles) in a pressure/flow graphic in figure 3. We start by increasing the mouth pressure until the reed suddenly shuts (point **A**). This immediately increases the pressure, so that the transition to region **B** is not represented in the graph (dashed arrow). We then decrease the pressure while the reed slightly opens until point **C**. Again the reed suddenly opens inducing a rapid transition to point **D**. The trajectory to zero pressure is then coincident with the beginning of the measurement.

In figure 3, we have also plotted a theoretical characteristic curve (thin line) correspondent to best fit of Ψ to the measured data. This curve corresponds to $\Psi = -2$.

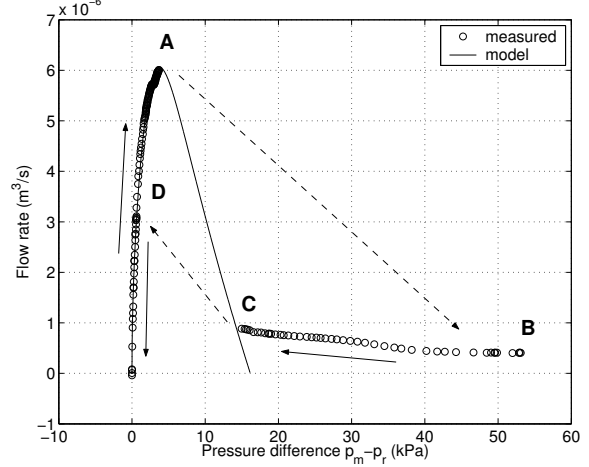While in [4] emphasis is given to the influence of a positive value of Ψ, the experimental data available at present needs a negative value of Ψ in order to be fitted to the static version of equations (1), (2) and (4).

4. Modeling

Real simulations require a suitable discretization of the equation set described in the previous section.

4.1. Discretization

4.1.1. Reed

A centered Euler discretization scheme is simple enough to get a set of algebraic equations which can be solved explicitly, as we shall see in section 4.2. It approximates better the solution at time t than the right-aligned Euler scheme, while allowing an explicit resolution (which the right-aligned Euler does not allow).

$$\frac{\partial z}{\partial t} \quad \rightarrow \quad \frac{1}{2}\left(z_{t+dt} - z_{t-dt}\right) \qquad (9)$$

$$\frac{\partial^2 z}{\partial t^2} \quad \rightarrow \quad z_{t+dt} - 2z_t + z_{t-dt} \qquad (10)$$

Equation 1 becomes:

$$(M + R)z'_{t+dt} - 2Mz'_t + (M - R)z'_{t-1}$$
$$- K(H' - z'_t)^\alpha - p'_t + p'_m = 0 \qquad (11)$$

While discretizing equation 1, we also replace the parameters by non-dimensional values, so that all the terms appearing in equation 11 are of order 1. In the latter we have:

- $M = \frac{m}{dt^2}\frac{1}{k}$; $\qquad R = \frac{r}{dt}\frac{1}{k}$; $\qquad K = 1$

- Primes (y') represent dimensionless values of a physical variable or parameter

4.1.2. Flow

The flow equation 2 does not need to be discretized but we rewrite it with non-dimensioned values:

$$\begin{aligned} q'_t &= B_1 z'_t \sqrt{|p'_m - p'_t|} \\ &= \text{sign}(p'_m - p'_t) \end{aligned} \tag{12}$$

with $B_1 = 1$ after adimensionalization.

4.1.3. Resonator

The discretization of the equation for a generic resonator (5) can be written as:

$$\sum_{i=0}^{N} P_i \frac{kH}{P_0} p'_{t-idt} = \sum_{j=0}^{M} Q_j \frac{k\alpha l_r}{P_0} \left(\frac{2kH}{\rho} \right)^{1/2} q'_{t-jdt} \tag{13}$$

In the present model this discretization uses a right-aligned Euler scheme.

The coefficients of p' and q' are dimensionless so that both the variables and the terms have an order of magnitude of 1.

4.2. Solution

z'_t can be computed before the other variables, since it only depends on past values of those. The solution is given by equation 11 by replacing t by $t - dt$. It is possible that at some point in the simulation this equation might give a negative value for the reed position. This is physically impossible because $z'_t = 0$ corresponds to a shut reed. In such a case the reed position is forced to $z'_t = 0$ and the solution for the other two equations (12 and 13) is trivial.

4.3. Real-time model

The model described in the former paragraphs is simple enough to be implemented in real time environments such as *pd* [^2]. We use *pd* to test different versions of the model and to quickly test the influence of newly introduced terms in the flow (2) or reed (1) equations.

The measured values of the stiffness law and Ψ coefficient were introduced in the real-time *pd* model. Although the difference from a single reed model can be perceived by scanning the appropriate range of parameters, the effect is difficult to demonstrate graphically because the variation of timbre can be more important within a model than between the two models for a similar parameter set.

The effect of the negative Ψ coefficient is an overall gain in brilliance of the sound, while the power law for

[^2]: Pure-Data is a real-time graphical programming environment for audio and graphical processing. See http://www.pure-data.org

the stiffness seems to soften the attacks and decays of the sound.

5. Conclusion

Present real-time simulations presented in this article are not suitable for the sound synthesis of a real double-reed instrument, due to the excessive simplification of some important parts of the instrument (such as the resonator). However, the parallel approach of gathering experimental data and testing it in a real-time model speeds up the testing for relevance of the phenomena identified in the experiments: relevant details of the model produce qualitative changes in the behavior of the model and in the sound it produces.

By completing the measurements hereby presented, and extending them to non-static regimes we expect to improve the quality of the reed model. We will refine the resonator model using the same implementation principles but including theoretical and experimental data already existent in the literature. This will hopefully allow us to propose an interesting double-reed model for sound synthesis.

References

[1] A. Almeida, C. Vergez, R. Caussé, and X. Rodet. Etude des écoulements dans les instruments à vent à anche double, pour application à la synthèse par modèle physique. In *CFA, Congrès Français d'Acoustique*, Lille, France, 2002.

[2] A. Almeida, C. Vergez, and R. Caussé. Experimental investigations on double reed quasi-static behavior. In *ICA 2004*, 2004.

[3] A. P. J. Wijnands and A. Hirschberg. Effect of a pipe neck downstream of a double reed. In *Proceedings of the International Symposium on Musical Acoustics*, pages 149–152. Societe Française d'Acoustique, 1995.

[4] C Vergez, A. Almeida, R. Causse, and X. Rodet. Toward a simple physical model of double-reed musical instruments: Influence of aero-dynamical losses in the embouchure on the coupling between the reed and the bore of the resonator. *Acustica*, 2003.

[5] A. Almeida, C. Vergez, R. Caussé, and X. Rodet. Physical study of double-reed instruments for application to sound-synthesis. In *International Symposium in Musical Acoustics*, Mexico, Mexique, December 2002.

[6] J. P. Dalmont, J. Gilbert, and S. Ollivier. Nonlinear characteristics of single-reed instruments: quasi-static volume flow and reed opening measurements. *Journ. Acoust. Soc. of Amer.*, 114(4):2253–2262, October 2003.